

A improved equation of state for Xe gas bubbles in γ U-Mo fuels

Benjamin Beeler^{a,*}, Shenyang Hu^b, Yongfeng Zhang^a, Yipeng Gao^a

^a*Idaho National Laboratory, Idaho Falls, ID 83415*

^b*Pacific Northwest National Laboratory, Richland, WA 99354*

Abstract

A monolithic fuel design based on a U-Mo alloy has been selected as the fuel type for conversion of the United States High-Performance Research Reactors (HPRRs). An issue with U-Mo monolithic fuel is the large amount of swelling that takes place during operation. The accurate prediction of fuel evolution under irradiation requires implementation of correct thermodynamic properties into mesoscale and continuum level fuel performance modeling codes. However, the thermodynamic properties of the bubbles (such as the relationship among bubble size, equilibrium Xe concentration, and bubble pressure) are not well known. This work studies Xe bubbles in γ U-Mo from a diameter of 2 nm up to 7 nm and from 400 K up to 700 K. The energetic relationship of Xe bubbles with regard to voids and Xe substitutional atoms is described. The transition is also determined for when a bubble becomes over-pressurized. Finally, an equation of state is fit to the pressure as a function of molar volume and temperature.

1. Introduction

The United States High-Performance Research Reactor (USHPRR) program targets replacing current highly enriched uranium (HEU) fuel in high power research reactors with low enriched uranium (LEU) fuel [1]. In order to achieve a reduced enrichment in these fuel types, there is the requirement for increased
5 uranium density. One way this is achieved is by utilizing γ stabilized uranium alloys with 10 wt.% or less alloy content. The fuel design being pursued under the USHPRR program is a uranium-molybdenum (U-Mo) monolithic foil, with a zirconium (Zr) diffusion barrier in Al clad.

An issue with U-Mo monolithic fuel is the large amount of swelling that takes place during operation[2]. Such swelling needs to be stable and predictable up to high fission densities. Research reactor fuel types
10 based on U-Mo are unique in their ability to stably retain fission gases to high fission densities, and as such there is a relatively high content of fission gas and of fission gas bubbles within the fuel matrix. The importance of swelling in addition to the unique fuel environment has led to a variety of experimental studies characterizing the swelling behavior in U-Mo fuels [3, 4, 5, 6] which has led to the development of a swelling correlation as a function of fission density from Argonne National Labortory (ANL correlation) [7] and Idaho
15 National Laboratory [8]. A 2015 post-irradiation examination (PIE) report [9] from Williams, et al. showed

*Corresponding author

Email address: benjamin.beeler@inl.gov (Benjamin Beeler)

higher swelling in U-10Mo fuels at fission densities much lower than previously observed. This accelerated fuel swelling behavior could lead to early fuel failure and was not captured by the ANL correlation. As such, a more mechanistic fuel swelling model is needed in order to predict swelling behavior of U-Mo fuels under both typical operating conditions, as well as transients, accident scenarios and different reactor environments.

Recently, substantial effort has been made on mesoscale models to describe the swelling behavior of U-Mo fuels [10, 11, 12, 13, 14, 15, 16, 17]. These models rely on phase-field and/or rate theory descriptions of material systems in order to model swelling on realistic timescales on a microstructural level. These simulation methodologies include a number of parameters that are either fit to limited experimental data, calculated from lower length scale modeling methodologies, or assumed based on other material systems. However, the thermodynamic properties of the bubbles (such as the relationship among bubble size, equilibrium Xe concentration, and bubble pressure) are not well known. Implementation of correct thermodynamic properties into mesoscale and continuum level fuel performance modeling codes is crucial for the accurate prediction of fuel evolution under irradiation, particularly in regard to swelling.

Xiao, et al. [18, 19] studied U-Mo-Xe bubbles of less than 2 nm in diameter, analyzing the pressure and induced swelling with increasing Xe content. They also modeled bubble coalescence as a function of temperature. They observed interesting effects such as a decrease in bubble pressure and Xe density with increasing number of Xe atoms in present in the bubble. The origin of such anomalous effects is unclear. Recently, Hu developed an equation of state of Xe bubbles in U-Mo at 500 K by determining Xe density and pressure [20]. They also studied dislocation emission from fission gas bubbles and suggested a possible cause of the face-centered cubic fission gas superlattice due to the tensile stress surrounding the bubbles. However, this work was restricted to a single temperature and very small bubbles of diameter less than 2 nm. Although this is typically the size of bubbles found in the fission gas superlattice [7], after grain refinement the superlattice bubbles coalesce and form much larger bubbles, up to 1 micron in diameter [9]. The inclusion of only small, highly pressurized bubbles into an equation of state that governs all possible Xe bubble configurations excludes a significant amount of information. Therefore, it is valuable to extend the previous work that was performed to investigate much larger systems and a wider variety of Xe concentrations within bubbles in order to incorporate as much information as possible to facilitate mesoscale models of fission gas swelling and microstructural evolution in U-Mo fuels.

This work studies Xe bubbles in γ -U-Mo from a diameter of 2 nm up to 7 nm and from 400 K up to 700 K. The energetic relationship of Xe bubbles with regard to voids and Xe substitutional atoms is described. The transition is also determined for when a bubble becomes over-pressurized. Finally, an equation of state is fit to the pressure as a function of molar volume and temperature.

2. Computational Details

Molecular dynamics simulations are performed utilizing the LAMMPS [21] software package and the U-Mo-Xe embedded atom method (EAM) interatomic potential [22]. A supercell of 40x40x40 body-centered

cubic (bcc) unit cells (128,000 U atoms) is generated, and approximately 22 percent of U atoms are randomly switched to Mo atoms, yielding a U-10Mo (10 weight percent) alloy in the bcc structure. Relaxation of the bulk system is performed in an NPT-ensemble, relaxing each x, y, and z component individually, with a damping parameter of 0.1. A Langevin thermostat in the Gronbech-Jensen-Farago [23, 24] formalism is
55 utilized with the damping parameter set to 0.01 ps. Temperatures of interest are 400 K, 500 K, 600 K and 700 K, which span the realistic operating temperatures for U-Mo fuels. The system is allowed to equilibrate for 100 ps at a given temperature, and subsequently a void is constructed by deleting a sphere of atoms from the center of the supercell. This void is relaxed for 100 ps under the same simulation conditions described above.

60 In order to analyze bubbles, two sets of simulations are performed: an NPT and an NVT ensemble. An NVT ensemble is utilized to mimic a bubble in a very large system that effectively exerts a resistive pressure on the bubble. This allows for the calculation of a Xe bubble pressure and a subsequent equation of state based on the density of the bubble. The NPT ensemble allows the system volume to change and to determine the transition between an under-pressurized bubble, where the volume of the system is less than
65 the equilibrium volume of a U-10Mo alloy, to an over-pressurized bubble, where the volume of the system is greater than the equilibrium volume of a U-10Mo alloy. The target pressure for the NPT ensemble is 0.

The generation of bubbles is performed by inserting Xe atoms into the void one at a time, while relaxation of the system is ongoing. For smaller bubbles, the insertion rate is as low as one Xe atom per 5 ps. For the largest voids/bubbles investigated, the insertion rate is higher, with one Xe atom inserted every 2 ps. In order
70 to track the bubble size, two atoms (one on either side of the void) are tracked throughout the simulation and the distance between the two atoms is classified as the diameter of the bubble. The pressure of the bubble is determined by computing the stress per atom on each of the Xe atoms in the system, summing the individual components of the stress tensor over all Xe atoms and finally dividing by the degrees of freedom (three) and the volume of the bubble.

75 The equation of state (EOS) for Xe bubbles is taken from Kaplun [25], which was also utilized in the work of Hu [20],

$$P = \frac{RT}{v} \left(1 + \frac{c}{v-b} \right) - \frac{a}{v^2} \quad (1)$$

where R is the gas constant for Xe (8.253 J/mol-K[25]), T is the temperature in K, P is the pressure in MPa, v is the molar volume in cm³/mol, and a, b, and c are fitting parameters. This EOS reduces to the well known Van der Waals EOS when b=c. It appears that Hu [20] mislabeled the fitting parameters in their
80 equation, as the units do not match the equation. Thus, it is our interpretation that the EOS parameters from Hu are a=259,780 J-cm³/mol², b=18.928 cm³/mol and c= 280.658 cm³/mol. These parameters are utilized as the starting guess for the fitting procedure in this work to obtain an optimized EOS.

A minimization script is utilized to fit the EOS to the determined pressure and molar volume data from the molecular dynamics simulations. The data is input into the script, and the squared error is summed and

utilized to optimize the EOS, iterating by providing a random step to each of the a, b and c coefficients and only accepting the iteration if the summed error is reduced.

3. Results

In order to generate bubbles in the methodology outlined above, voids of varying size must be generated. This allows for the calculation of a void surface area as a function of radius, and the surface energy can be determined from equation 2

$$E_{surf} = \frac{(E^* - E)}{A} \times N \quad (2)$$

where E^* is the potential energy per atom of the system with a void, E is the potential energy per atom of the perfect crystal of U-Mo, A is the total surface area of the void and N is the number of atoms in the system with a void. The void surface energy is shown in Fig. 1. It should be emphasized that all of these systems are random solid substitutional alloys of U-10Mo in an NVT ensemble unless specifically mentioned otherwise. It can be observed that the void surface energy converges above a radius of 20 Å for all temperatures to a value of approximately 1.2 J/m². This is similar in magnitude to, albeit slightly lower than, the average surface energy for U-Mo free surfaces as determined in [26], which utilized an Angular-Dependent potential [27] capable of describing the U-Mo system. It is expected that different interatomic potentials would yield different values for the void surface energy. However, this calculation gives confidence that voids are reaching a relaxed, converged state to provide a foundation for insertion of Xe atoms to create bubbles.

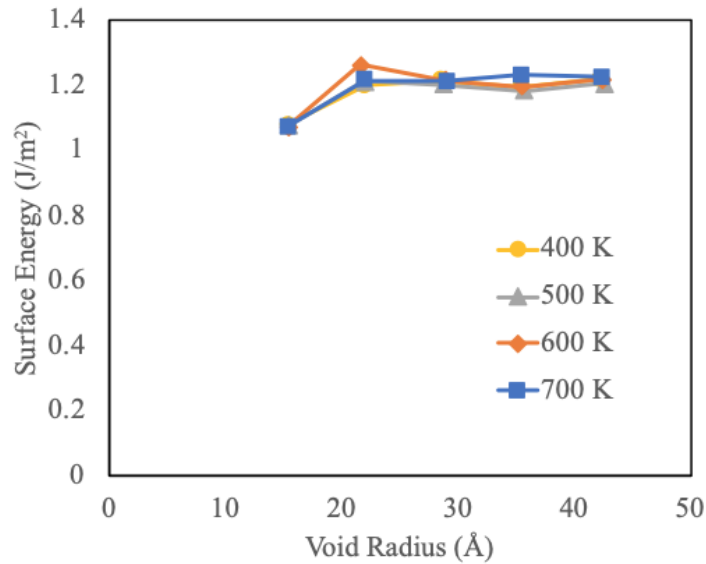


Figure 1: Void surface energy as a function of radius for voids in U-10Mo from 400 K to 700 K.

An example bubble is shown in Fig. 2. Atoms are progressively inserted into a void, leading to an increasing Xe to vacancy ratio as a function of simulation time, resulting in a highly pressurized Xe bubble at the end of the simulation. The maximum Xe/vacancy ratio obtained varies as a function of bubble radius, due primarily to the energetic relationships observed in U-Mo-Xe bubbles, and secondarily due to computational expense.

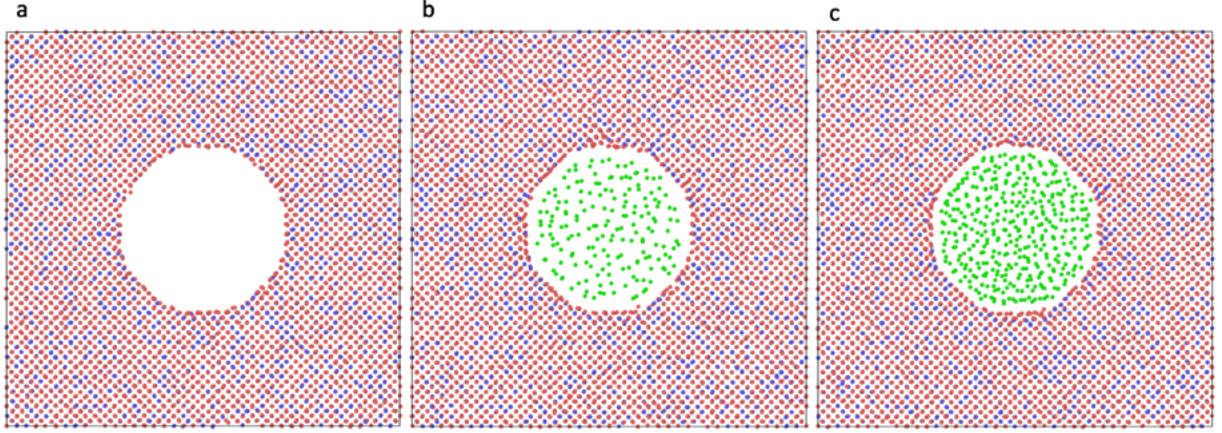


Figure 2: A Xe bubble at 500 K with a diameter of 7.1 nm in U-10Mo as a function of time. Starting from a void (a), to a Xe/vacancy ratio of 0.16 (b), and a Xe/vacancy ratio of 0.32 (c). Red atoms are U, blue atoms are Mo and green atoms are Xe.

The bubble formation energy can be calculated by the following equation:

$$E_f^{bub} = E^{bub} - \frac{N^{void}}{N^{sys}} E^{sys} \quad (3)$$

where E^{bub} is the energy of the system with a bubble, N^{void} is the number of atoms in the system with a void, E^{sys} is the energy of the bulk system (no voids or bubbles) and N^{sys} is the number of atoms in the bulk system. The energy per atom of Xe in its reference state is neglected in this calculation, as the energy is sufficiently small (< 0.1 meV/at) to result in only statistically insignificant changes to formation energies. In order to compare different bubble sizes to one another, a relative bubble energy is defined as the bubble formation energy less the void formation energy. With this formalism, only the excess energy attributable to the Xe atoms and their subsequent influence on the energy of the system is analyzed. This allows for the investigation of energetic effects of Xe bubbles for different bubble sizes. The relative bubble energy at 500 K is shown in Fig. 3 for bubbles of diameter 1.7, 3.1, 4.4, 5.8 and 7.1 nm.

For all bubbles, there is a region below a Xe/vacancy ratio of 0.15 where additional Xe atoms inserted into the bubble produce no noticeable change in the relative bubble energy. There can even exist a slight reduction in system energy due to Xe aiding in the faceting of the low pressure bubble. Above a Xe/vacancy ratio of approximately 0.15, the relative bubble energy displays a quadratic increase as a function of the Xe/vacancy ratio. The specific nature of the quadratic growth is dependent upon the bubble size, where a larger bubble displays a more rapid increase in relative bubble energy. This shows that it is much more

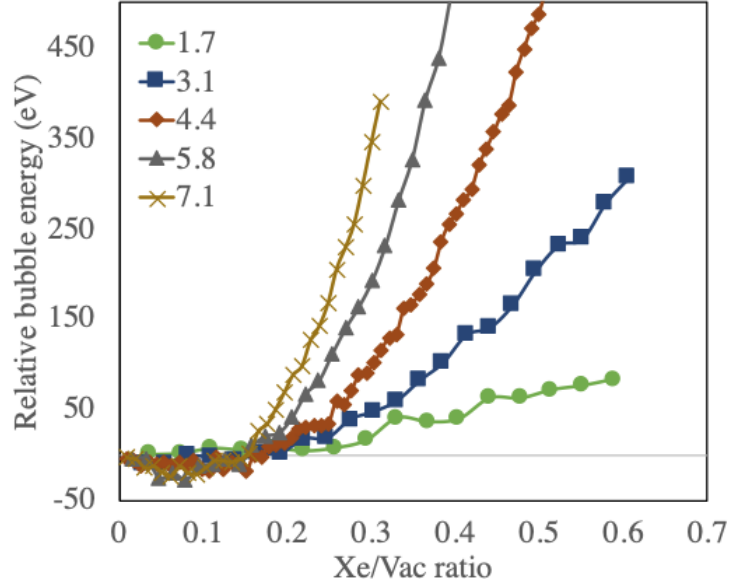


Figure 3: Relative bubble energy at 500 K as a function of Xe/vacancy ratio for bubbles of five unique sizes. Bubble diameters labeled, units in nm.

difficult to obtain a high Xe/vacancy ratio in large bubbles compared to small bubbles.

The energetic preference for adding or removing a Xe atom into an existing bubble can be investigated by looking at the binding energy of the n th Xe atom in a given bubble. The binding energy of the n th Xe atom in a given bubble can be defined as:

$$E^{bind} = E(n) - E(n-1) - E_{Xe}^{int} \quad (4)$$

where $E(n)$ is the energy of system a bubble with n Xe atoms, $E(n-1)$ is the energy of system a bubble with $n-1$ Xe atoms and E_{Xe}^{int} is the formation energy of a Xe substitutional-vacancy pair. The formation energy of a Xe sub-vac defect is determined to be 5.2 eV. This is a likely isolated Xe defect complex, as this defect structure is lower in energy than a Xe interstitial (6.2 eV) or a Xe substitutional (5.6 eV). The binding energy of the n th Xe atom in a given bubble is shown in Fig. 4, for all bubble sizes investigated. It is shown that the binding energy is negative for all Xe/vacancy ratios included in this study, illustrating that it is always favorable for a Xe atom to reside in a bubble, regardless of existing Xe/vacancy ratio, rather than to reside in the bulk U-Mo alloy. The binding energy does grow less strong with increasing Xe/Vac ratio, as would be expected, but there is no observed scenario where it is energetically favorable for a Xe atom to reside in the bulk instead of as an atom in the bubble. Extrapolating a quadratic fit to a binding energy of zero yields a Xe/Vac ratio of 1.1. It should be noted that data for all bubble sizes is included in this graph as there is no observable difference in Xe binding energy as a function of Xe/Vac ratio.

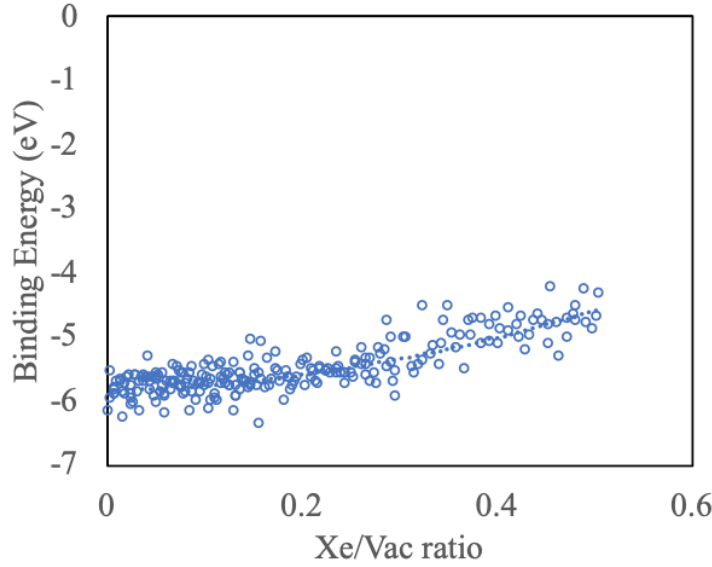


Figure 4: Binding energy of the n th Xe atom in a bubble as a function of the Xe/vacancy ratio.



In order to determine the under- to over-pressurized transition, simulations in an NPT ensemble at 500 K are performed to allow the volume to change as a function of time. The equilibrium volume of a U-10Mo alloy is determined prior to the introduction of a void and subsequent introduction of Xe atoms. A relaxed system with a void exhibits a reduced volume compared to the equilibrium system. As Xe is introduced into the void/bubble, the Xe exerts an outward force on the system. As progressively more Xe is added into the bubble, the pressure becomes significant enough to expand the bulk system and increase the supercell volume. This work defines the transition from under- to over-pressurized bubbles as the point where the volume of the system with a Xe bubble is equal to the equilibrium volume of a system with no void or bubble. Thus, at a lower Xe/vacancy ratio, the system will have a slightly lower volume than the equilibrium system, and at a higher Xe/vacancy ratio the system will have a slightly higher volume than the equilibrium system. The results are shown in Fig. 5. The system becomes over-pressurized at different Xe/vacancy ratios depending upon the bubble diameter. For smaller bubbles, the transition occurs at a higher Xe/vacancy ratio. However, for the bubbles investigated, the range of variance for all bubble sizes is somewhat small. The transition occurs as early as a 0.19 Xe/vacancy ratio for a bubble of diameter 7.1 nm, and as late as a 0.26 Xe/vacancy ratio for a bubble of diameter 1.7 nm. Proceeding the transition, the volume increase is related to the size of the bubble as well, as larger bubbles see significantly more rapid volume increase with a given increase in the Xe/vacancy ratio. Particularly for large bubbles, a decrease in volume can be observed for low Xe content, this is due to faceting of the bubbles, induced by thermal motion of Xe atoms within bubble, as previously mentioned.

An equilibrium bubble can be understood as the bubble existing at the under- to over-pressurized transition. Typically the pressure of such a bubble is determined by satisfying the Young-Laplace equation, often

denoted by equation 5.

$$P = \frac{2\gamma}{R} \quad (5)$$

where γ is the surface energy and R is the radius of the bubble. Although the Young-Laplace equation was formulated to describe the interface across fluids, it is commonly used to describe gas bubbles in solids. To verify if the Young-Laplace relationship holds for Xe bubbles in UMo, the Xe/Vac ratio satisfying equation 5 is calculated and compared to the results from Fig. 5. The results agree impressively, in that from equation 5 the predicted equilibrium bubble Xe/Vac ratios vary from 0.22 to 0.29, with a decrease in the equilibrium Xe/Vac ratio with increasing bubble radius. Thus, it is stipulated that the Young-Laplace relationship holds for Xe bubbles in UMo and the equilibrium pressure can be obtained, given the surface energy and the bubble radius.

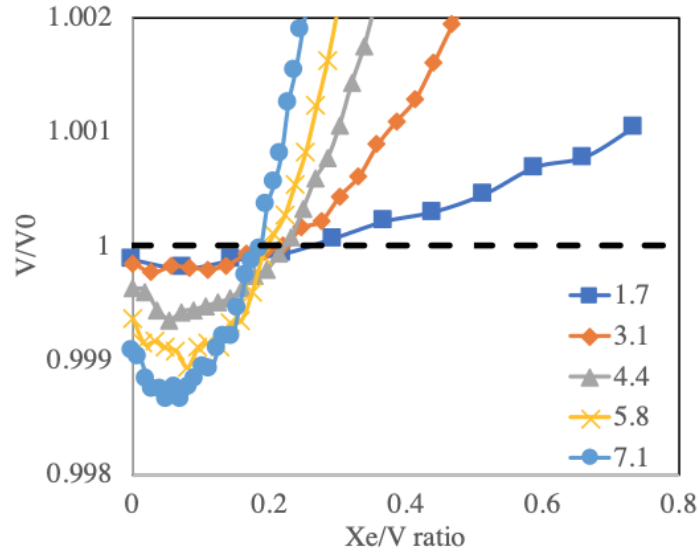


Figure 5: The relative volume of a system with a bubble as a function of Xe/vacancy ratio for five unique bubble sizes. Bubble diameters labeled, units in nm.

I might need to remake this figure which the proper data I find. I calculated numbers for 400 K, in the 400C folder

Finally, the equation of state can be determined by tracking the pressure inside the bubble and the bubble size as a function of the number of Xe atoms present in the bubble while the system is equilibrated in an NVT ensemble, which provides a pressure versus density relationship. In order to extend the applicability of the EOS, temperatures from 400 K to 700 K are analyzed, for all bubble radii previously mentioned. Equation 1 is used to fit pressure versus molar volume information, and the subsequent fit, with included molecular dynamics data, is shown in Fig. 6. An inlay is included for molar volumes from 20 to 80 cc/mol, to better illustrate the high pressure data. The data heavily overlaps and only shows minor differences as a function

of temperature and as such the individual isotherms are difficult to distinguish. As such, the MD data is removed in Fig. 7 and the optimized EOS is displayed on a log/linear scale to emphasize the differences between the individual isotherms. The optimized coefficients for the equation of state are $a=40,000 \text{ J}\cdot\text{cm}^3/\text{mol}^2$, $b=18.03 \text{ cm}^3/\text{mol}$, $c=445.01 \text{ cm}^3/\text{mol}$. Compared to the work of Hu, this is a significant decrease in the parameter a , a similar value in b , and a substantial increase in c . The root-mean squared deviation (RMSD) over the entire data set is 829 MPa (note that the maximum pressure in the dataset is 7.4 GPa). Since the range of pressures in this dataset covers multiple orders of magnitude, it can be better to investigate error with a normalized RMSD (NRMSD). One way of constructing a NRMSD is by dividing the RMSD by the range (the difference of the maximum and minimum) of the dataset. In this way, the NRMSD of the optimized EOS compared to the MD data is 13%. Considering that the pressure in this dataset varies over 3 orders of magnitude and the temperature varies over 300 K, this is reasonable agreement. The RMSD and the NRMSD of the previously optimized EOS from Hu is calculated with respect to the MD data in this work, with observed deviations of 1234 MPa and 20%, respectively. Thus, this represents approximately a 7% improvement over the most finely calibrated EOS for Xe bubbles in UMo in the literature, as well as a dramatic expansion on the range of applicability, with respect to bubble size, pressure and temperature.

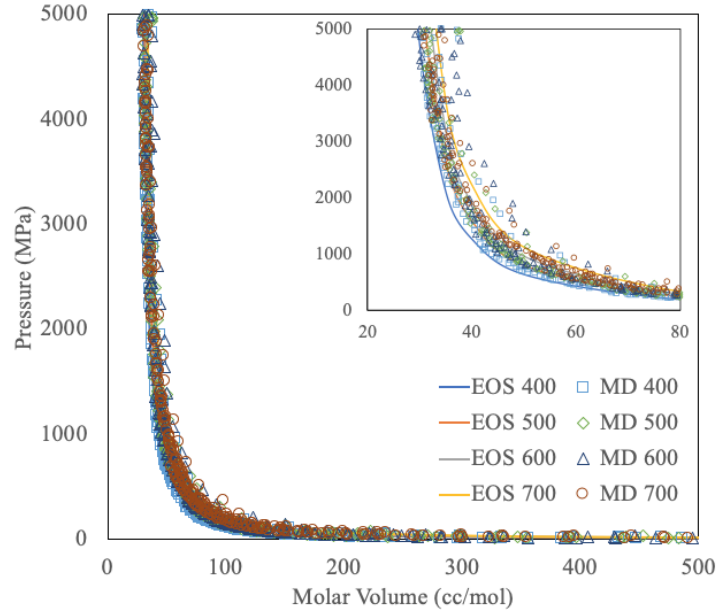


Figure 6: An equation of state (EOS) for Xe bubbles in U-10Mo from 400 K to 700 K compared to molecular dynamics data.

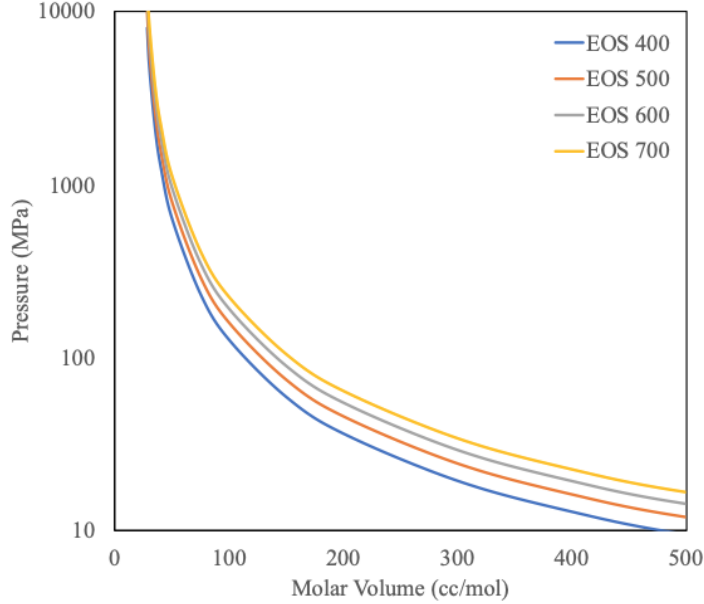



Figure 7: Four isotherms of the optimized equation of state (EOS) for Xe bubbles in U-10Mo. Axes are presented on a log/linear scale to emphasize differences in the individual isotherms.

4. Conclusions

This work investigated Xe bubbles in γ U-Mo from a diameter of 2 nm up to 7 nm and from 400 K up to 700 K.. The energetic relationship of Xe bubbles with regard to voids and Xe interstitial atoms is described. The relative energy of a bubble increases quadratically as a function of Xe/vacancy ratio, with larger bubbles exhibiting a more rapid increase in energy. The binding energy of Xe atoms is negative, indicating attraction, for all bubbles and all Xe/vacancy ratios investigated. This shows that the energy of a Xe atom in the UMo lattice is sufficiently high, such that Xe will always want to reside in the bubble, regardless of bubble pressure. The transition is determined for when a bubble becomes over-pressurized. This transition is below a Xe/vacancy ratio 0.25 for all bubbles in this work.  ally, an equation of state was fit to the pressure as a function of molar volume and temperature for Xe in UMo bubbles. This new EOS represents an improvement in accuracy and extended applicability compared to a previously developed EOS.

The knowledge that the Xe/vacancy ratio depends on the bubble size and optimally decreases with increasing bubble diameter is valuable, in that the assumption is typically made of a constant Xe/vacancy ratio, regardless of bubble size. Also, the examined Xe/vacancy ratios in this study are somewhat lower than the previous estimate of fission gas densities in bubbles in U-Mo, although the pressures are similar in magnitude. The information provided in this work regarding bubble energetics, under- to over-pressurization transition, and an updated equation of state for Xe bubble in U-10Mo can be directly utilized to improve the fidelity of mesoscale models that describe fission gas induced swelling in U-Mo fuels.

5. Acknowledgement

This work was supported by the U.S. Department of Energy, Office of Material Management and Minimization, National Nuclear Security Administration, under DOE-NE Idaho Operations Office Contract DE-AC07-05ID14517. This manuscript has been authored by Battelle Energy Alliance, LLC with the U.S. Department of Energy. The publisher, by accepting the article for publication, acknowledges that the U.S. Government retains a nonexclusive, paid-up, irrevocable, worldwide license to publish or reproduce the published form of this manuscript, or allow others to do so, for U.S. Government purposes. This research made use of the resources of the High Performance Computing Center at Idaho National Laboratory, which is supported by the Office of Nuclear Energy of the U.S. Department of Energy and the Nuclear Science User Facilities.

6. References

- [1] J. Snelgrove, G. Hofman, M. Meyer, C. Trybus, T. Weincek, Development of very-high density low enriched uranium fuels, Nucl. Eng. Design 178 (1997) 119.
- [2] G. Hofman, L. Walters, T. Bauer, Metallic fast reactor fuels, Progress in Nuclear Energy 31 (1997) 83.
- [3] J. Rest, G. Hofman, Y. Kim, Analysis of intergranular fission-gas bubble-size distributions in irradiated uranium-molybdenum alloy fuel, J. Nucl. Mater. 385 (2009) 563.
- [4] Y. Kim, G. Hofman, J. Rest, G. Shevlyakov, Characterization of intergranular fission gas bubbles in u-mo fuel, Tech. Rep. ANL-08/11, Argonne National Laboratory (2008).
- [5] M. Meyer, G. Hofman, S. Hayes, C. Clark, T. Wiencek, J. Snelgrove, R. Strain, K. Kim, Low-temperature irradiation behavior of uranium-molybdenum alloy dispersion fuel, J. Nucl. Mater. 304 (2002) 221.
- [6] Y. Kim, G. Hofman, J. Cheon, A. Robinson, D. Wachs, Fission induced swelling and creep of u-mo alloy fuel, J. Nucl. Mater. 437 (2013) 37.
- [7] Y. Kim, G. Hofman, Fission product induced swelling of u-mo alloy fuel, J. Nucl. Mater. 419 (2011) 291.
- [8] M. Meyer, B. Rabin, J. Cole, I. Glagolenko, W. Jones, J.-F. Jue, J. D. Keiser, C. Miller, G. Moore, H. Ozaltun, F. Rice, A. Robinson, J. Smith, D. Wachs, W. Williams, N. Woolstenhulme, Preliminary report on u-mo monolithic fuel for research reactors, Tech. Rep. INL/EXT-17-40975, Idaho National Laboratory (2017).
- [9] W. Williams, F. Rice, A. Robinson, M. Meyer, B. Rabin, Afip-6 mkii post-irradiation examination summary report, Tech. Rep. INL/LTD-15-34142, Idaho National Laboratory (2015).

- [10] L. Liang, Y. Kim, Z.-G. Mei, L. Aagesen, A. Yacout, Fission gas bubbles and recrystallization-induced degradation of the effective thermal conductivity in u-7mo fuels, *J. Nucl. Mater.* 511 (2018) 438.
- 245 [11] L. Liang, Z.-G. Mei, Y. Kim, M. Anitescu, A. Yacout, Three-dimensional phase-field simulations of intragranular gas bubble evolution in irradiated u-mo fuel, *Comp. Mat. Sci.* 145 (2018) 86.
- [12] L. Liang, Z.-G. Mei, A. Yacout, Fission-induced recrystallization effect on intergranular bubble-driven swelling in u-mo fuel, *Comp. Mat. Sci.* 138 (2017) 16.
- 250 [13] L. Liang, Z.-G. Mei, Y. Kim, B. Ye, G. Hofman, M. Anitescu, A. Yacout, Mesoscale model for fission-induced recrystallization in u-7mo alloy, *Comp. Mat. Sci.* 124 (2016) 228.
- [14] B. Ye, G. Hofman, A. Leenaers, A. Bergeron, V. Kuzminov, S. V. den Berghe, Y. Kim, H. Wallin, A modelling study of the inter-diffusion layer formation in u-mo/al dispersion fuel plates at high power, *J. Nucl. Mater.* 499 (2018) 191.
- 255 [15] S. Hu, V. Joshi, C. Lavender, A rate-theory-phase-field model of irradiation-induced recrystallization in umo nuclear fuels, *JOM* 69 (2017) 2554.
- [16] S. Hu, D. Burkes, C. Lavender, V. Joshi, Effect of grain morphology on gas bubble swelling in umo fuels – a 3d microstructure dependent booth model, *J. Nucl. Mater.* 480 (2016) 323.
- [17] S. Hu, D. Burkes, C. Lavender, D. Senior, W. Setyawan, Z. Xu, Formation mechanism of gas bubble superlattice in umo metal fuels: Phase-field modeling investigation, *J. Nucl. Mater.* 479 (2016) 202.
- 260 [18] H.-X. Xiao, R. Tang, X.-F. Tian, C.-S. Long, Molecular dynamics simulation of xe behavior in u-mo alloys fuel, *Chin. Phys. Lett.* 31 (2014) 047101.
- [19] H.-X. Xiao, C.-S. Long, X.-F. Tian, S. Li, Atomistic simulations of the small xenon bubble behavior in u-mo alloy, *Materials and Design* 74 (2015) 55.
- 265 [20] S. Hu, W. Setyawan, V. Joshi, C. Lavender, Atomistic simulations of thermodynamic properties of xe gas bubbles in u10mo fuels, *J. Nucl. Mater.* 490 (2017) 49.
- [21] S. Plimpton, Fast parallel algorithms for short-range molecular dynamics, *J. Comp. Phys.* 117 (1995) 1–19.
- [22] D. Smirnova, A. Kuksin, S. Starikov, V. Stegailov, Z. Insepov, J. Rest, A. Yacout, A ternary eam interatomic potential for u-mo alloys with xenon, *Modelling Simul. Mater. Sci. Eng.* 21 (2013) 035011.
- 270 [23] N. Gronbech-Jensen, O. Farago, A simple and effective verlet-type algorithm for simulating langevin dynamics, *Mol. Phys.* 111 (2013) 983.
- [24] N. Gronbech-Jensen, N. Hayre, O. Farago, Application of the g-jf discrete-time thermostat for fast and accurate molecular simulations, *Comp. Phys. Comm.* 185 (2014) 524.

- [25] A. Kaplun, A. Meshalkin, Thermodynamic validation of the form of unified equation of state for liquid and gas, *High Temperature* 41 (2003) 319.
- [26] B. Beeler, Y. Zhang, Y. Gao, An atomistic study of grain boundaries and surfaces in gamma u-mo, *J. Nucl. Mater.* 507 (2018) 248.
- [27] D. Smirnova, A. Kuksin, S. Starikov, V. Stegailov, Atomistic modeling of the self-diffusion in gamma u and gamma u-mo, *Phys. Met. and Metall.* 116 (2015) 445.